Carnegie Observatories Astrophysics Series, Vol. 2:
Measuring and Modeling the Universe, 2004
ed. W. L. Freedman (Pasadena: Carnegie Observatories,
http://www.ociw.edu/ociw/symposia/series/symposium2/proceedings.html)

The Latest Version of the Standardized Candle Method for Type II Supernovae

M. HAMUY
The Observatories of the Carnegie Institution of Washington

Abstract
I use the largest available sample of Type II plateau supernovae to examine the previously reported luminosity-velocity relation. This study confirms such relation which permits one to standardize the luminosities of these objects from a spectroscopic measurement of their envelope velocities, and use them as extragalactic distance indicators. The "standard candle method" (SCM) yields a Hubble diagram with a dispersion of 0.3 mag, which implies that the SCM produces distances with a precision of 15%. Using two nearby supernovae with Cepheid distances I find H_0=81±10 km s^{-1} Mpc^{-1}, which compares with H_0=74 derived from Type Ia supernovae.

1.1 Introduction

Type II supernovae (SNe II, hereafter) are exploding stars characterized by strong hydrogen spectral lines and their proximity to star forming regions, presumably resulting from the gravitational collapse of the cores of massive stars (M_{ZAMS}>8 $M_\odot$). SNe II display great variations in their spectra and lightcurves depending on the properties of their progenitors at the time of core collapse and the density of the medium in which they explode (Hamuy 2003a). The plateau subclass (SNe IIP) constitutes a well-defined family which can be distinguished by 1) a characteristic "plateau" lightcurve (Barbon et al. 1979), 2) Balmer lines exhibiting broad P-Cygni profiles, and 3) low radio emission (Weiler et al. 2002). These SNe are thought to have red supergiant progenitors that do not experience significant mass loss and are able to retain most of their H-rich envelopes before explosion.

Although SNe IIP display a wide range in luminosity, rendering their use as standard candles difficult, Hamuy & Pinto (2002) (HP02, hereafter) recently used a sample of 17 SNe II to show that their plateau luminosities are well correlated with the expansion velocities of their ejecta, which implies that the luminosities can be standardized from a spectroscopic measurement of the SN ejecta velocity. This "standard candle method" (SCM) affords a new opportunity to derive independent and potentially precise extragalactic distances. In this paper I use a larger sample of 24 SNe IIP to assess the precision of the SCM and solve for the Hubble constant based on two SNe with Cepheid distances.

1.2 The Luminosity-Velocity Relation

I collected published and unpublished photometric and spectroscopic data for the largest possible sample of SNe IIP in order to re-evaluate the luminosity-velocity relation. The current sample comprises 24 SNe IIP, 15 of which were included in the HP02 list.

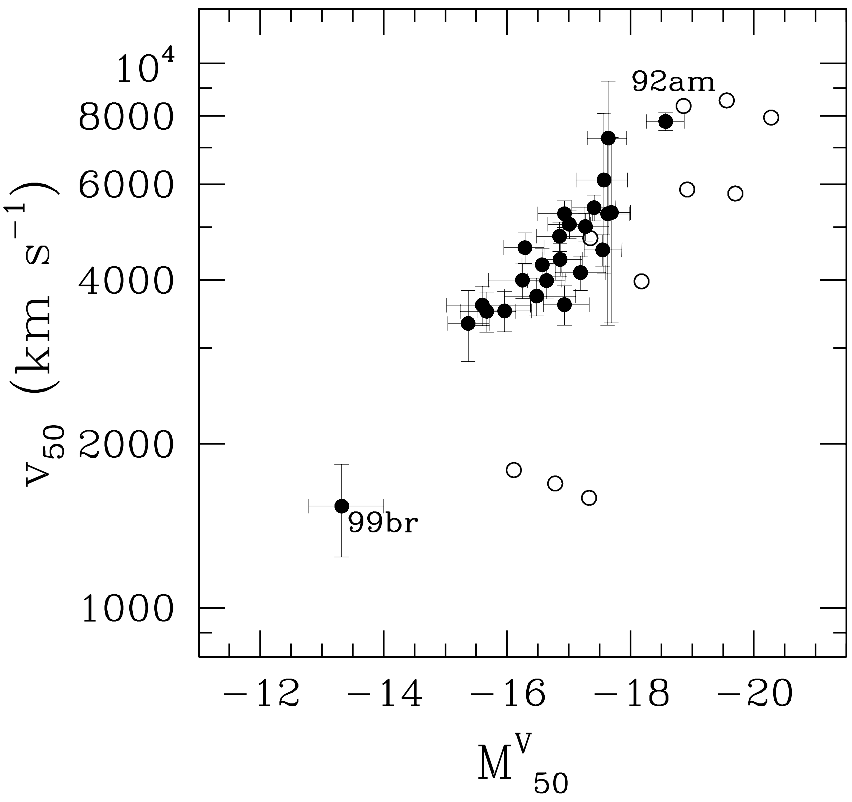

Fig. 1.1. Expansion velocities from Fe II λ5169 versus absolute *V* magnitude, both measured in the middle of the plateau (day 50) of 24 SNe IIP (filled circles) and the models of LN83 and LN85 with $\geq 8\ M_\odot$ (open circles).

Here I exclude SN 1987A and SN 2000cb from the HP02 sample for exhibiting non-plateau lightcurves.

I measured apparent magnitudes 50 days after explosion (nearly the middle of the plateau phase) for the 24 SNe IIP, I applied corrections to the observed fluxes using my best estimate for dust extinction (see next section), and converted the fluxes into luminosities from redshift-based distances corrected for the peculiar motion of the Galaxy and the SN host galaxy (using the flow model described in the next section). Also, I measured ejecta velocities from the minimum of the Fe II λ5169 lines, and I interpolated them to the same epoch (50 days after explosion) by fitting a power-law to the observed velocities following the precepts described by Hamuy 2001.

Figure **??** compares the plateau *V* luminosity and ejecta velocity for these 24 SNe IIP (filled circles) which reveals the well-known fact that SNe IIP encompass a wide range (∼5 mag) in luminosities, and confirms the luminosity-velocity relation previously reported by HP02. The extreme objects in this diagram are the dim and low-velocity SN 1999br and the luminous high-velocity SN 1992am. This result reflects the fact that while the explosion energy increases, so do the kinetic energy and internal energies. Also plotted in this figure with open circles are the models of Litvinova & Nadezhin (1983, 1985) (hereafter LN83 and LN85) for SNe with progenitors masses $\geq 8\ M_{\odot}$, which reveals a reasonable agreement with observations.

1.3 Determination of Dust Extinction

In order to use astronomical objects as standard candles it proves necessary to correct the observed fluxes for dust absorption. The estimate of Galactic extinction is under good control thanks to the IR dust maps of Schlegel et al. (1998), which permit one to estimate $A_{GAL}(V)$ to ± 0.06 mag. The determination of absorption in the host galaxy, on the other hand, is not so straightforward.

Here I explore a method which assumes that SNe IIP should all reach the same color toward the end of the plateau phase, so a measurement of the color should give directly the color excess due to dust absorption. The underlying assumption is that the opacity in SNe IIP is dominated by e^- scattering, so they should all reach the same temperature of hydrogen recombination toward the end of the plateau phase (Eastman et al. 1996).

Next I proceed to test this method using the best-studied plateau SN 1999em as the reference for the intrinsic color. For this purpose I adopt the $A_{host}(V)$=0.18 value derived by Baron et al. (2000) from detailed theoretical modeling of the spectra of SN 1999em. For the other SNe I use their $B-V$ and $V-I$ color at the end of the plateau phase to determine the color offset relative to SN 1999em and the corresponding visual extinction, $A_{host}(V)$, assuming the extinction law of Cardelli et al. (1989) for R_V=3.1.

The technique is illustrated in Figure **??**. The top panels show with filled circles the $B-V$ color curves of SN 1999cr (left) and SN 1999gi (right) corrected for Galactic extinction, after applying an offset in order to match the dereddened color curves of SN 1999em (crosses). The required offset for each SN is indicated in units of visual extinction A_V. The bottom panels show the same procedure using $V-I$ colors.

Table **??** gives the results for all 24 SNe. An inspection of this table reveals that the $B-V$ method has serious problems since in 10 cases it yields negative reddenings. This is particularly pronounced among the historical SNe, reaching $A_{host}(V)$=-1.2 for SN 1970G. It is possible that part of the problem is due to inadequate transformations of the photographic magnitudes into the standard Johnson system, or to background contamination by the host galaxy. However, even SN 1999cr (with modern CCD photometry) yields a negative value of $A_{host}(V)$=-0.75 (Fig. **??**), which is well beyond the photometric errors. The $V-I$ method produces independent reddenings for 17 SNe. This method is much well behaved: only SN 1992af yields a modest negative reddening of $A_{host}(V)$=-0.2.

Figure **??** compares the $A_{host}(V)$ values obtained from $B-V$ and $V-I$ which reveals serious discrepancies between both methods. It is possible that the problem is due to metallicity effects which are stronger in the B band where line blanketing is more pronounced (Eastman et al. 1996, Baron et al. 2003). In any case, this is an unsatisfactory situation and other techniques should be explored in the future.

Although the $V-I$ method should be preferred owing to the smaller sensitivity to metallicity effects, in what follows I use the average of the $B-V$ and $V-I$ extinction values (or

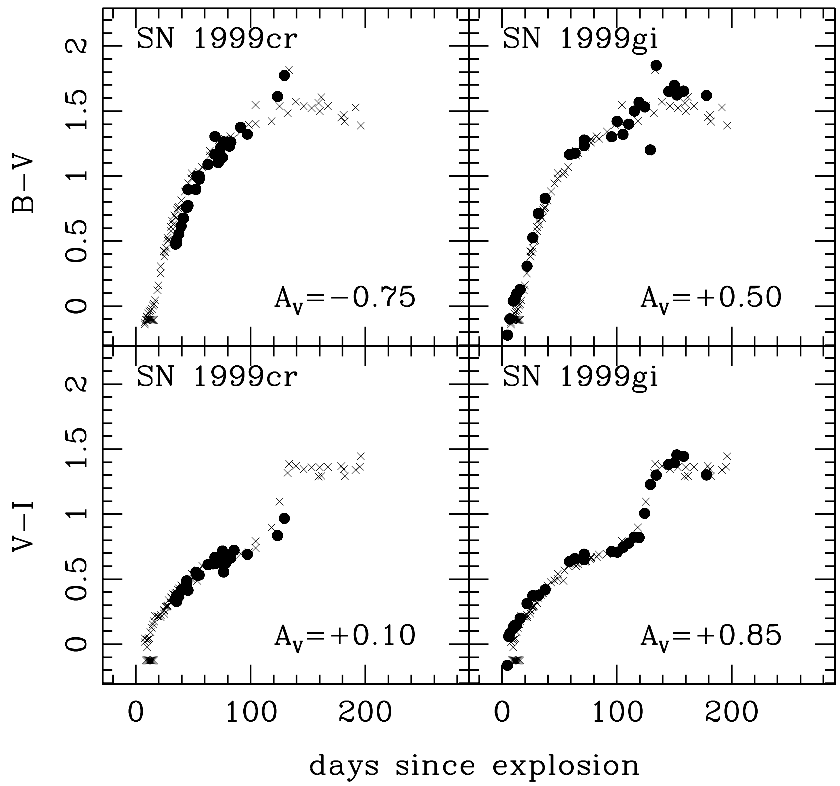

Fig. 1.2. (Top) With filled circles are shown the $B-V$ color curves of SN 1999cr (left) and SN 1999gi (right) corrected for Galactic extinction, and after applying a color offset in order to match the dereddened color curves of SN 1999em (crosses). The required offset for each SN is indicated in each panel in units of visual extinction A_V. (Bottom) Same as above but for $V-I$. This figure shows that, while the offsets required for SN 1999gi agree quite well and probably reflect dust extinction in the host galaxy, the required offsets for SN 1999cr reveal a poor agreement.

the single-color value when only one color is available) since I do not have $V-I$ colors for all SNe. The resulting $A_{host}(V)$ values are listed in Table **??** to which I assign an uncertainty of ±0.3 mag based on the reddening difference yielded by both methods.

1.4 The Hubble Diagram

In a uniform and isotropic Universe we expect locally a linear relation between distance and redshift. A perfect standard candle located at different distances should describe a straight line in the magnitude-log(z) Hubble diagram, so the observed scatter is a measure of how standard the candle is, which is what I proceed to assess for the SCM.

Table 1.1. *Galactic and Host-galaxy Extinction for 24 Type II Supernovae.*

SN	$A_{GAL}(V)$ ($\pm$0.06)	$A_{host}(V)$ $(B-V)$	$A_{host}(V)$ $(V-I)$	$A_{host}(V)$ ($\pm$0.3)
1968L	0.219	-0.90	...	0.00
1969L	0.205	-0.70	...	0.00
1970G	0.028	-1.20	...	0.00
1973R	0.107	1.40	...	1.40
1986I	0.129	...	0.20	0.20
1986L	0.099	0.30	...	0.30
1988A	0.136	-0.40	...	0.00
1989L	0.123	-0.60	0.90	0.15
1990E	0.082	1.00	1.90	1.45
1990K	0.047	0.05	0.35	0.20
1991al	0.168	-0.30	0.10	0.00
1991G	0.065	...	0.00	0.00
1992H	0.054	0.00	...	0.00
1992af	0.171	-0.40	-0.20	0.00
1992am	0.164	0.35	0.20	0.28
1992ba	0.193	-0.15	0.15	0.00
1993A	0.572	0.00	0.10	0.05
1993S	0.054	1.00	0.40	0.70
1999br	0.078	0.50	0.80	0.65
1999ca	0.361	0.85	0.50	0.68
1999cr	0.324	-0.75	0.10	0.00
1999eg	0.388	-0.15	0.05	0.00
1999em	0.130	0.18	0.18	0.18
1999gi	0.055	0.50	0.85	0.68

For the 8 most distant SNe (cz>3000 km s^{-1}) I used the observed heliocentric redshifts of their host galaxies, either from the NASA/IPAC Extragalactic Database or my own measurement (Hamuy 2001), and converted them to the Cosmic Microwave Background (CMB) frame in order to remove the observer's peculiar motion. In these cases I neglected the peculiar motion of the hosts since they are small compared to their cosmological redshifts. In the remaining cases this effect is potentially significant so I attempted to correct it using the parametric model for peculiar flows of Tonry et al. (2000). In this model the CMB velocity of a galaxy is given by

$$\mathbf{v_{CMB}} = H_0\ \mathbf{D_{SBF}} + \mathbf{v_{pec}}, \tag{1.1}$$

where $\mathbf{D_{SBF}}$ is the SBF distance of Tonry et al. (2001) in the Ferrarese et al. (2000) scale (F00), $\mathbf{v_{pec}}$ is the peculiar velocity of the galaxy which is a function of $\mathbf{D_{SBF}}$ and galactic coordinates, and H_0 is the Hubble constant which has a value of 78.4 km s^{-1} Mpc^{-1}.

For 9 galaxies I used $\mathbf{v_{CMB}}$ and inverted equation **??** to solve for $\mathbf{D_{SBF}}$, from which the velocity component free of peculiar motion, H_0 $\mathbf{D_{SBF}}$, could be trivially computed. In 5

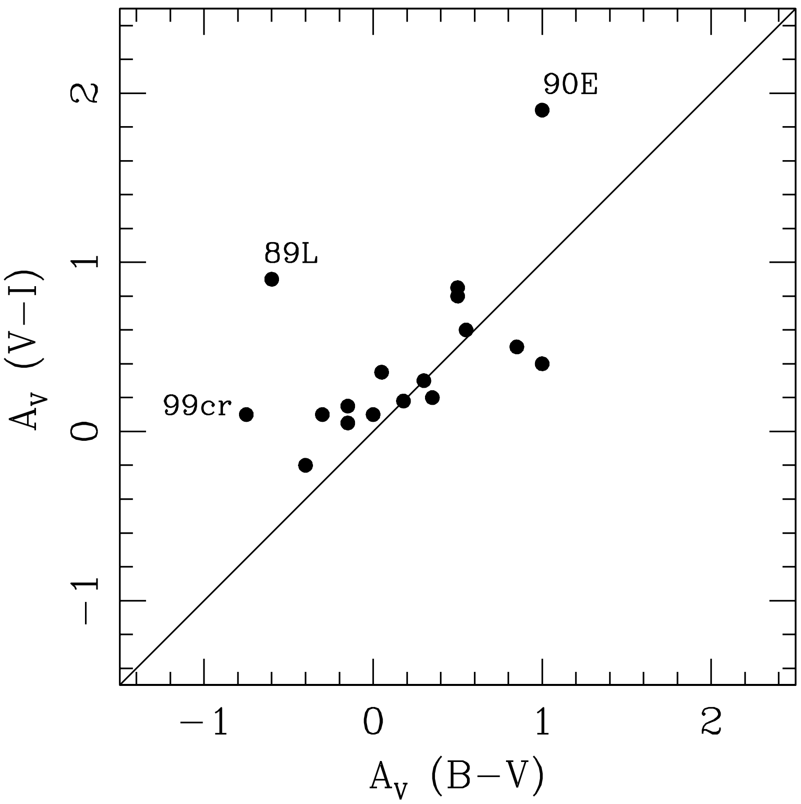

Fig. 1.3. Comparison between host-galaxy visual absorption extinction (A_V) of SNe IIP from $B-V$ and $V-I$ color curves. The ridge line is the 45° line and not a fit to the data.

cases it was possible to assign the SN host to a galaxy group and use the corresponding SBF distance given by Tonry et al. (2001) to compute H_0 $\mathbf{D_{SBF}}$ directly. In two cases I used Cepheid distances in the F00 scale. The resulting redshifts are listed in Table **??** for the 24 SNe. In all cases I assigned an uncertainty of $\pm$187 km s^{-1}, which corresponds to the cosmic thermal velocity yielded by the model for peculiar flows.

The other ingredients for the Hubble diagram are the apparent magnitudes and the ejecta velocities of the SNe. A convenient choice (but not the only one) is to use magnitudes in the middle of the plateau, so I interpolated the observed V and I fluxes to the time corresponding to 50 days after explosion. Other parameterizations might yield better results and should be explored in the future. The ejecta velocities come from the minimum of the Fe II λ5169 lines interpolated to day 50 (as described in Hamuy 2001), which is good to $\pm$300 km s^{-1}. In 4 cases it was necessary to extrapolate velocities so I adopted a greater uncertainty of $\pm$2000 km s^{-1}. The magnitudes and velocities are given in Table **??** for all SNe.

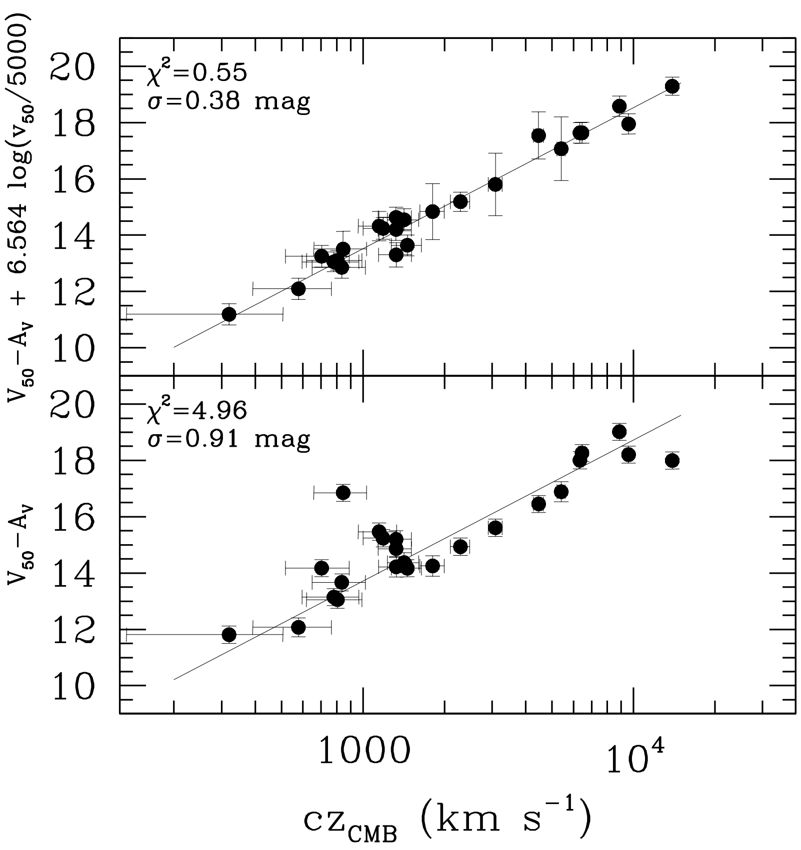

Fig. 1.4. (bottom) Raw Hubble diagram from SNe II plateau V magnitudes. (top) Hubble diagram from V magnitudes corrected for envelope expansion velocities.

The bottom panel of Figure **??** shows the Hubble diagram in the V band, after correcting the apparent magnitudes of Table **??** for the reddening values in Table **??**, while the top panel shows the same magnitudes after correction for expansion velocities. A least-squares fit to the data in the top panel yields the following solution,

$$V_{50} - A_V + 6.564(\pm 0.88)\, log(v_{50}/5000) = 5\, log(cz) - 1.478(\pm 0.11). \tag{1.2}$$

The scatter drops from 0.91 mag to 0.38 mag, thus demonstrating that the correction for ejecta velocities standardizes the luminosities of SNe IIP significantly. It is interesting to note that part of the spread comes from the nearby SNe which are potentially more affected by peculiar motions of their host galaxies. When the sample is restricted to the eight objects with cz>3,000 km s^{-1}, the scatter drops to only 0.33 mag. The corresponding fit for the restricted sample is,

$$V_{50} - A_V + 6.249(\pm 1.35)\, log(v_{50}/5000) = 5\, log(cz) - 1.464(\pm 0.15). \tag{1.3}$$

Table 1.2. *Redshifts, Magnitudes, and Ejecta Velocities of the 24 Type II Supernovae.*

SN	v_{CMB} ($\pm$187 km s^{-1})	Redshift Source[a]	V_{50}	I_{50}	v_{50} (km s^{-1})
1968L	321	1	12.03(08)	...	4020(300)
1969L	784	1	13.35(06)	...	4841(300)
1970G	580	2	12.10(15)	...	5041(300)
1973R	808	2	14.56(05)	...	5092(300)
1986I	1333	1	14.55(20)	14.05(09)	3623(300)
1986L	1466	3	14.57(05)	...	4150(300)
1988A	1332	1	15.00(05)	...	4613(300)
1989L	1332	3	15.47(05)	14.54(05)	3529(300)
1990E	1426	3	15.90(20)	14.56(20)	5324(300)
1990K	1818	3	14.50(20)	13.90(05)	6142(2000)
1991al	4484	4	16.62(05)	16.16(05)	7330(2000)
1991G	1152	1	15.53(07)	15.05(09)	3347(500)
1992H	2305	3	14.99(04)	...	5463(300)
1992af	5438	4	17.06(20)	16.56(20)	5322(2000)
1992am	14009	4	18.44(05)	17.99(05)	7868(300)
1992ba	1192	3	15.43(05)	14.76(05)	3523(300)
1993A	8933	4	19.64(05)	18.89(05)	4290(300)
1993S	9649	4	18.96(05)	18.25(05)	4569(300)
1999br	848	3	17.58(05)	16.71(05)	1545(300)
1999ca	3105	4	16.65(05)	15.77(05)	5353(2000)
1999cr	6376	4	18.33(05)	17.63(05)	4389(300)
1999eg	6494	4	18.65(05)	17.94(05)	4012(300)
1999em	838	3	13.98(05)	13.35(05)	3757(300)
1999gi	706	3	14.91(05)	13.98(05)	3617(300)

[a]Code:
1: $\mathbf{v_{CMB}}$=H_0 $\mathbf{D_{SBF}}$, where $\mathbf{D_{SBF}}$ is SBF distance and H_0=78.4.
2: $\mathbf{v_{CMB}}$=H_0 $\mathbf{D_{Ceph}}$, where $\mathbf{D_{Ceph}}$ is Cepheid distance and H_0=78.4.
3: CMB redshift corrected for peculiar flow model of Tonry et al. (2000).
4: Heliocentric redshift corrected to CMB.

Figure **??** shows the same analysis but in the I band. In this case the scatter in the raw Hubble diagram is 0.83 mag, which drops to 0.32 mag after correction for ejecta velocities. This is even smaller that the 0.38 spread in the V band, possibly due to the fact that the effects of dust extinction are smaller at these wavelengths. The least-squares fit yields the following solution,

$$I_{50} - A_I + 5.869(\pm 0.68)\, log(v_{50}/5000) = 5\, log(cz) - 1.926(\pm 0.09). \tag{1.4}$$

When the eight most distant objects are employed the spread is 0.29 mag, similar to that obtained from the V magnitudes and the same sample, and the solution is,

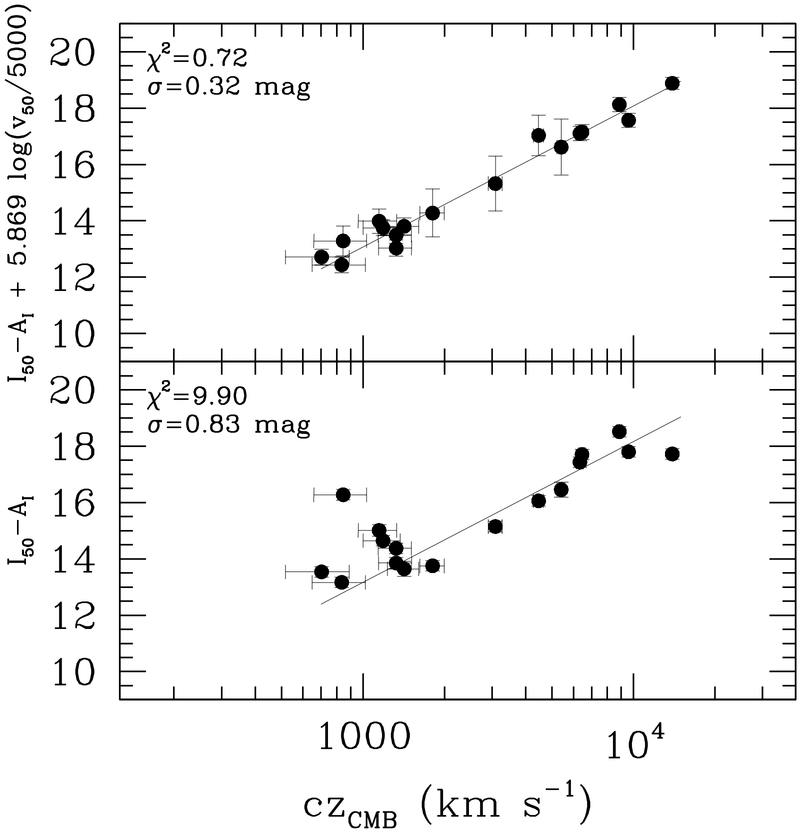

Fig. 1.5. (bottom) Raw Hubble diagram from SNe II plateau *I* magnitudes. (top) Hubble diagram from *I* magnitudes corrected for envelope expansion velocities.

$$I_{50} - A_I + 5.445(\pm 0.91)\, log(v_{50}/5000) = 5\, log(cz) - 1.923(\pm 0.11). \tag{1.5}$$

This analysis shows that the SCM can produce relative distances with a precision of 15%, but more objects in the Hubble flow are required to pin down the actual precision of this technique.

1.5 The Value of the Hubble Constant

The SCM can be used to solve for the Hubble constant, provided a distance calibrator is available. If the distance D of the calibrator is known, the Hubble constant is given by

$$H_0(V) = \frac{10^{V_{50} - A_V + 6.249 log(v_{50}/5000) + 1.464}}{D}, \tag{1.6}$$

when the distant sample is adopted. A similar expression applies to the I band data.

Among the objects of our sample SN 1968L, SN 1970G, SN 1973R, and SN 1999em have precise Cepheid distances, but only two of them have been published so far (Freedman et al. 2001). The distances and the corresponding H_0 values are summarized in Table **??**. Within the uncertainties the two estimates are in good agreement, and the average proves to be 81±10 km s^{-1} Mpc^{-1}. This result compares with the 74 value derived from Type Ia SNe calibrated in the Freedman et al. (2001) scale (M. M. Phillips, this meeting), which lends further credibility to the SCM.

Table 1.3. *The Hubble Constant.*

SN	Distance Modulus	$H_0(V)$ (km s^{-1} Mpc^{-1})
1970G	29.13(11)	77±13
1973R	29.86(08)	87±15
Average		81±10

HP02 found a value of H_0=55±12 based on one calibrator (SN 1987A), which proves significantly lower than the current 81±10 value. The main reason for this difference is that SN 1987A is not a plateau event and should not have been included in the HP02 sample since the physics of its lightcurve is different than that of SNe IIP. Unlike these objects which have red supergiants progenitors (Arnett 1996, Hamuy 2003b), SN 1987A exploded as a compact blue supergiant (Woosley et al. 1987) and most of the energy deposited in the envelope by the shock wave formed after core collapse went into adiabatic expansion, thus leading to a dimmer plateau and to a lightcurve promptly powered by ^{56}Ni → ^{56}Co → ^{56}Fe (Blinnikov et al. 2000).

The Cepheid distances for SN 1968L and SN 1999em will be released soon (G. Tammann and D. Leonard, priv. comm.), thus improving significantly the H_0 value from the SCM. SN 1999em will prove particularly important because it has far better observations than any of the other 3 calibrators, both in the V and I bands.

1.6 Conclusions

I used the largest possible sample of SNe IIP to examine their use as standardized candles. The main conclusions of this study are the following,
1) The luminosity-velocity relation previously reported by HP02 is confirmed from this larger sample of 24 SNe.
2) The luminosity-velocity relation can be used to standardize the luminosities of SNe IIP, and the corresponding Hubble diagram has a dispersion of 0.3 mag, which implies that SNe IIP can produce distances with a precision of 15%.
3) Using two nearby SNe with Cepheid distances I find a value of H_0=81±10, which compares with the 74 value derived from Type Ia SNe.
4) The least satisfactory aspect of the SCM is the dereddening method based on the SN color curves, which produces different results depending on the color used. Clearly other techniques need to be explored in the future.
4) This study confirms that SNe IIP offer a great potential as distance indicators. These con-

clusions, however, are based on several historical SNe with poor photometric observations and few objects in the quiet Hubble flow. Clearly a greater sample of SNe with $cz > 3000$ km s^{-1} and modern CCD photometry is needed. The recently launched Carnegie Supernova Program at Las Campanas Observatory has already targeted a dozen such SNe and in the next two years it will produce an unprecedented database of spectroscopy and optical/infrared photometry for a large number of SNe, which will allow us to achieve this goal.
5) Although the precision of the SCM is only half as good as that produced by SNe Ia, with the 8-m class telescopes currently in operation it should be possible to get spectroscopy of SNe IIP down to $V\sim23$ and start populating the Hubble diagram up to $z\sim0.3$. A handful of SNe IIP will allow us to check the distances to SNe Ia.

Acknowledgements. I dedicate this work to my dear friends and collaborators Bob Schommer and Marina Wischnjewsky, for their tireless work which led to an enormous progress of the supernova field over recent years. Support for this work was provided by NASA through Hubble Fellowship grant HST-HF-01139.01-A awarded by the Space Telescope Science Institute, which is operated by the Association of Universities for Research in Astronomy, Inc., for NASA, under contract NAS 5-26555.

References

Arnett, D. 1996, Supernovae and Nucleosynthesis (New Jersey: Princeton Univ. Press)
Barbon, R., Ciatti, F., & Rosino, L. 1979, A&A, 72, 287
Baron, E., et al. 2000, ApJ, 545, 444
Baron, E., Nugent, P. E., Branch, D., Hauschildt, P. H., Turatto, M. & Cappellaro, E. 2003, ApJ, 586, 1199
Blinnikov, S., Lundqvist, P., Bartunov, O., Nomoto, K., & Iwamoto, K. 2000, ApJ, 532, 1132
Cardelli, J. A., Clayton, G. C., & Mathis, J. S. 1989, ApJ, 345, 245
Eastman, R. G., Schmidt, B. P., & Kirshner, R. 1996, ApJ, 466, 911
Ferrarese, L., et al. 2000, ApJ, 529, 745 (F00)
Freedman, W. L., et al. 2001, ApJ, 553, 47
Hamuy, M. 2001, Ph.D. thesis, Univ. Arizona
——. 2003a, in Core Collapse of Massive Stars, ed. C. L. Fryer (Dordrecht: Kluwer), in press (astro-ph/0301006)
——. 2003b, ApJ, 582, 905
Hamuy, M., & Pinto, P. A. 2002, ApJ, 566, L63 (HP02)
Litvinova, I. Y., & Nadezhin, D. K. 1983, Ap&SS, 89, 89 (LN83)
——. 1985, SvAL, 11, 145 (LN85)
Schlegel, D. J., Finkbeiner, D. P., & Davis, M. 1998, ApJ, 500, 525
Tonry, J. L., et al. 2001, ApJ, 546, 681
Tonry, J. L., Blakeslee, J. P., Ajhar, E. A., & Dressler, A. 2000, ApJ, 530, 625
Weiler, K. W., Panagia, N., Montes, M. J., & Sramek, R. A. 2002, ARA&A, 40, 387
Woosley, S. E., Pinto, P. A., Martin, P. G., & Weaver, T. A. 1987, ApJ, 318, 664